Atmos. Chem. Phys. Discuss., https://doi.org/10.5194/acp-2018-22
Manuscript under review for journal Atmos. Chem. Phys.
Discussion started: 22 January 2018

Atmospheric Chemistry and Physics Discussions

Simulation of Atmospheric Organic Aerosol using its Volatility-Oxygen Content Distribution during the PEGASOS 2012 campaign

Eleni Karnezi[a], Benjamin N. Murphy[b], Laurent Poulain[c], Hartmut Herrmann[c], Alfred Wiedensohler[c], Florian Rubach[c,d,e], Astrid Kiendler-Scharr[d], Thomas F. Mentel[d] and Spyros N. Pandis[a,f,g*]

[a] *Department of Chemical Engineering, Carnegie Mellon University, Pittsburgh, USA*
[b] *National Exposure Research Laboratory, United States Environmental Protection Agency, Research Triangle Park, North Carolina, USA*
[c] *Leibniz Institute for Tropospheric Research, Permoserstr 15, 04318 Leipzig, Germany*
[d] *Institut fur Chemie und Dynamik der Geosphare, ICG, Forschungszentrum Julich, Julich, Germany*
[e] *Max Planck Institute for Chemistry, 55128 Mainz, Germany*
[f] *Department of Chemical Engineering, University of Patras, Patra, Greece*
[g] *Inst. of Chemical Engineering Sciences, FORTH/ ICEHT, Patra, Greece*

Abstract

A lot of effort has been made to understand and constrain the atmospheric aging of the organic aerosol (OA). Different parameterizations of the organic aerosol formation and evolution in the two-dimensional Volatility Basis Set (2D-VBS) framework are evaluated using ground and airborne measurements collected in the 2012 Pan-European Gas AeroSOls-climate-interaction Study (PEGASOS) field campaign in the Po Valley (Italy). A number of chemical aging schemes are examined, taking into account various functionalization and fragmentation pathways for biogenic and anthropogenic OA components. Model predictions and measurements, both at the ground and aloft, indicate a relatively oxidized OA with little average diurnal variation. Total OA concentration and O:C ratios were reproduced within experimental error by a number of chemical aging schemes. Anthropogenic SOA is predicted to contribute 15-25% of the total OA, while SOA from intermediate volatility compounds oxidation another 20-35%. Biogenic SOA contributions varied from 15 to 45% depending on the modeling scheme. Primary OA contributed to around 5% for all schemes and was comparable to the HOA concentrations of the PMF-AMS ground measurements. The average OA and O:C diurnal variation and their vertical profiles showed a surprisingly modest sensitivity to the assumed vaporization enthalpy for all aging schemes. This

can be explained by the intricate interplay between the changes in partitioning of the semi-volatile compounds and their gas-phase chemical aging reactions.

1. Introduction

Atmospheric aerosol plays an important role in the Earth's energy balance by absorbing and scattering solar radiation (direct effect) and influencing the properties and lifetime of clouds (indirect effects) (IPCC, 2014). At the same time, certain particles may have significant negative effects on human health, including premature death, increases in respiratory illnesses and cardiopulmonary mortality (Pope et al., 2009; Caiazzo et al., 2013).

Aerosol particles contain a wide variety of inorganic and organic compounds, with organics representing about 50% of the fine (< 1 μm) aerosol particle mass concentration, on average (Zhang et al., 2007). OA originates from many different natural and anthropogenic sources and processes. It can be emitted directly from fossil fuel and biomass combustion (so-called primary organic aerosol, POA) or can be formed by the atmospheric oxidation of organic vapors (secondary organic aerosol, SOA). The oxidation pathways of organic compounds are complex and the corresponding reactions lead to hundreds or even thousands of mostly unknown oxygenated products. As a result, our understanding of OA formation mechanisms and its chemical and physical properties remains incomplete.

The use of lumped species is a computationally efficient approach for the representation of OA in atmospheric chemical transport models (Pandis et al., 1992). The volatility basis set framework (VBS, Donahue et al., 2006) lumps these compounds into surrogates along an axis of volatility. This approach typically employs species with effective saturation concentrations at 298 K separated by one order of magnitude, with values ranging from, say, 0.01 to 10^6 μg m^{-3}. By quantifying the volatility distributions of primary and secondary OA, a physically reasonable, yet suitable for large-scale chemical transport models (CTMs), description of semi-volatile organics can be obtained (Lane et al., 2008).

The VBS framework was extended by Donahue et al. (2011; 2012a) adding another dimension, the oxygen content (expressed as the ratio of oxygen to carbon atoms; O:C), for the description of the OA chemical aging reactions. In the first application of this framework in a CTM, Murphy et al. (2011) used 12 logarithmically spaced volatility bins (effective saturation concentration C^* varying from 10^{-5} to 10^6 μg m^{-3} at 298 K) and 13 bins of O:C (from 0 to 1.2 with

a step of 0.1). In this way, 156 surrogate species were included in the model for each OA type. Five organic aerosol types were simulated separately: anthropogenic secondary organic aerosol (aSOA-v) produced during the oxidation of anthropogenic VOCs, biogenic secondary organic aerosol (bSOA), fresh primary organic aerosol (POA), secondary organic aerosol from the oxidation of semivolatile OA (SOA-sv) and SOA from the oxidation of intermediate volatility compounds (SOA-iv) as analytically described in Murphy et al. (2014).

Murphy et al. (2011; 2012) used a one-dimensional Lagrangian CTM (PMCAMx-Trj), as the host model for the simulations. PMCAMx-Trj simulates the chemical evolution of a column of air as it travels towards a user-selected receptor site. Three alternative parameterizations of the OA formation and chemical aging were evaluated using measurements of O:C and OA in three European sites (Murphy et al., 2011; 2012). The simplest approach parameterizing the chemical aging of anthropogenic compounds, assuming a net reduction of volatility by one bin during every aging reaction step accompanied by an increase of one or two oxygen atoms with an equal probability was the most successful. A more complex formulation of the chemical aging, assumed that functionalization was the only process taking place, and overpredicted the OA concentration while it underpredicted O:C in most cases. Adding fragmentation reactions together with the functionalization gave promising results, but it was clear that the various parameters of the scheme were not well constrained leading to large uncertainties in the simulation results, especially during summertime. Murphy et al. (2012) concluded that the 2D-VBS scheme that was used needs additional testing before it is ready for application in three-dimensional CTMs.

In Murphy and Pandis (2009; 2010) and Murphy et al. (2012) formation of significant bSOA during second and later generation aging reactions led to overestimation of OA concentration at both urban and rural sites. However, the first generation products of the oxidation of biogenic VOCs do continue to react in the atmosphere (Ng et al., 2006; Tritscher et al., 2011; Zhao et al., 2015; Szidat et al., 2006; Gilardoni et al., 2011; Yttri et al., 2011). The net effect on ambient bSOA levels of these chemical aging reactions remains uncertain.

Fragmentation of organic compounds during chemical aging is an important reaction pathway (Chacon-Madrid and Donahue, 2011; Murphy et al., 2011; Hermansson et al., 2014). During fragmentation reactions carbon bonds break, resulting in smaller compounds, which are more volatile than their precursors. A fragmentation probability, depending on O:C, has been used in the 2D-VBS framework (Donahue et al. 2011; 2012). A fragmentation probability, ranging from

0-0.4, has been used in the statistical oxidation model (SOM) that uses the carbon (C) and oxygen (O) atoms per compound as the independent variables (Cappa and Wilson, 2012). While the fragmentation pathways are clearly important for the OA levels, their parameterizations in existing models remain quite uncertain (Murphy et al., 2012).

The effect of temperature on the partitioning of OA components between the gas and particulate phases represents another source of uncertainty. Sheehan and Bowman (2001), concluded that a 10 ºC decrease in temperature can result in an increase of SOA by as much as 150% depending on the assumed vaporization enthalpy. This effect can theoretically lead to significant OA vertical gradients. Applying the 2D-VBS to FAME-08 in Finokalia, Greece, Murphy et al. (2011) reported low sensitivity of the OA concentration and O:C ratio measurements to the assumed vaporization enthalpy, with higher values leading to slightly lower O:C.

In this study, we evaluate different chemical aging mechanisms in the 2D-VBS approach focusing on the Po Valley in Italy. Extensive measurements were performed both at the ground and aloft from June 6 until July 8, 2012. Po Valley has major air quality problems due to both industrial and agricultural sources. A number of alternative chemical aging mechanisms are evaluated comparing the 2D-VBS predictions against the PEGASOS measurements. The role of bSOA chemical aging is explored. Finally, the sensitivity of the model to the assumed effective vaporization enthalpy is quantified in an effort to constrain this uncertain variable using the measurements aloft.

2. Lagrangian CTM Description

A one–dimensional Lagrangian chemical transport model (PMCAMx-Trj) (Murphy et al., 2011; 2012), simulating the air parcels that arrive at the desired receptor location, is used as the host for the 2D-VBS module. The model solves the general dynamic equation taking into account the following relevant atmospheric processes: atmospheric transport, gas and aqueous phase chemistry, dry and wet deposition of gases and aerosols and vertical turbulent dispersion together with area and point emissions. Ten computational cells are used to cover heights up to 3 km. The lowest cell has a height of 60 m. The SAPRC-99 (Carter, 2000) chemical mechanism is used for the simulation of gas–phase chemistry. The meteorological parameters (horizontal winds, temperature, pressure, vertical dispersion coefficients, water vapor, clouds, rainfall and land use) used as inputs in the model are provided by the Weather Research and Forecasting (WRF) model.

The WRF simulation was periodically re-initialized (every 3 days) to ensure the accuracy of the inputs to the CTM. Area and point emissions, both anthropogenic and biogenic, were also provided as hourly inputs for the European domain. The Global and regional Earth-system Monitoring using Satellite and in-situ data (GEMS) dataset (Visschedijk et al., 2007) is used for the emissions of anthropogenic gases. Anthropogenic emissions of organic and elemental carbon are based on the Pan-European Carbonaceous Aerosol Inventory developed during EUCAARI (Kulmala et al., 2009). Biogenic gridded emissions are produced from the combination of three different models. The Model of Emissions of Gases and Aerosols from Nature (MEGAN) provides the emissions from ecosystems (Guenther et al., 2006) and the O'Dowd et al. (2008) model provides the marine aerosol emissions. Finally, wildfire emissions are also included (Sofiev et al., 2008a, b). Details of the emission inventory used for Europe can be found in Fountoukis et al. (2011). In order to implement these emissions in our 2D-VBS model, we used the same volatility distribution of the emissions as in the original work (Fountoukis et al., 2011) and used the Murphy et al. (2012) methodology for mapping these to the 2D-VBS. Vertically resolved initial conditions and the top boundary conditions for PMCAMx-Trj were obtained from the corresponding output of the PMCAMx regional scale three-dimensional simulation for the same period.

2.1 Simulated periods

Six air parcels arriving at 3:00, 7:00, 11:00, 15:00, 19:00 and 23:00 local time (UTC+1) in the ground site of San Pietro Capofiume were simulated for a total of 7 days (15, 26, 27, and 28 of June and 4, 5 and 8 of July 2012). The air masses in the simulated trajectories originated all from Europe (mostly Portugal or France) or the Atlantic Ocean. We avoided days during which air masses originated from Africa since emission inventories for Africa are quite uncertain. We chose days for which the trajectories at the different altitudes originated all from the same region. The Hybrid Single Particle Lagrangian Integrated Trajectory HYSPLIT model (Draxler et al., 2009) was used to calculate 72 h back trajectories arriving at the receptor site. For consistency, we used the same WRF meteorological data as input to HYSPLIT to calculate the back trajectories. Following Murphy et al. (2011) we used the ensemble average of 20 trajectories with varied heights from 60 m up to 3 km.

The twenty 72 h HYSPLIT back trajectories arriving at San Pietro Capofiume at 3:00 LT on July 8, 2012 are shown in Figure 1 as an example. They all originated from the eastern Atlantic

Ocean, passed a day over the ocean and then travelled over Portugal and Spain for another day. The air masses continued over the Mediterranean Sea, Western Italy, and a few hours later arrived in the receptor site of San Pietro Capofiume. The HYSPLIT clustering analysis utility was used to estimate the average trajectory that was used in the simulations (Figure 1).

Zeppelin flights over Po Valley took place on 20, 21, 22 and 24 of June of 2012 and 1, 3 and 4 of July 2012. The HYSPLIT model was once again used to calculate trajectories arriving at the receptor site around Po Valley. All the flights took place between 4:00 LT until 13:00 LT. The flight path of the Zeppelin for June 4, 2012 is shown in Figure S1 as an example. The flight took place between 5:00 LT and 10:00 LT and the measurements took place in the nighttime boundary layer, the residual layer, but also in the mixed layer later in the day.

2.2 Chemical Aging Schemes

In our simulations, we considered three different functionalization schemes, two bSOA chemical aging parameterizations and explored the use of fragmentation mechanisms. These are summarized below.

2.2.1 Functionalization schemes

(a) Simple scheme

The first functionalization scheme (1-bin) used in our simulations was the simple scheme of Murphy et al. (2012) that had the best performance in the cases simulated in that study. In this scheme, there is one volatility bin reduction for every reaction with a simultaneous increase in oxygen atoms, with a probability of 50% for an increase of 1 oxygen atom and 50% probability for an increase of 2 oxygen atoms. The calculation of the O:C change from the number of added oxygen atoms is based on Donahue et al. (2011). The chemical aging reaction constants that are used for the reactions with OH are the same as in the base case of Murphy et al. (2011) with values equal to $1x10^{-11}$ cm^3 $molec^{-1}$ s^{-1} for anthropogenic SOA from VOCs (aSOA-v) and biogenic SOA (bSOA) and $4x10^{-11}$ cm^3 $molec^{-1}$ s^{-1} for SOA from semivolatile OA (SOA-sv) and intermediate volatility compounds (SOA-iv).

(b) Two-bin shift simple scheme

In the second functionalization scheme (2-bin), a two-volatility bin reduction is assumed for every reaction with a simultaneous increase in oxygen atoms. A 50% probability for the increase of 1 oxygen atom and 50% probability for the increase of 2 oxygen atoms are used. The calculation of the O:C shift in bins from the number of added oxygen atoms is based again on Donahue et al. (2011). This functionalization scheme assumes a more rapid reduction in volatility for every reaction and uses the same reaction constants for the reactions with OH as in the base case of Murphy et al. (2011).

(c) Detailed scheme

The third aging scheme is the detailed functionalization scheme (DET) introduced by Donahue et al. (2011). This is a more rigorous scheme compared to the previous two conservative aging parameterizations. Following Murphy et al. (2012), there is a 30% probability of adding one O atom, 50% probability of adding two O atoms, and 20% probability of adding three O atoms. Each addition of O atoms results in a different distribution of volatility reductions, with an average reduction of -1.75 in $\log_{10}C^*$ per oxygen group added. These additions of O atoms are translated to changes of O:C ratios following Murphy et al. (2012). The functionalization kernel is applied to all species in the 2D-VBS upon OH reaction. Again the chemical aging reaction constants that are used for the reaction with OH are the same as the two functionalization schemes described above.

2.2.2 bSOA aging parameterizations

Two different parameterizations of bSOA aging are explored. In the first scheme, the chemical aging of biogenic SOA is assumed to result in a negligible net change in volatility but an increase in O:C (Murphy et al., 2011). This scheme is consistent with the lack of bSOA aging that has been used in PMCAMx (Murphy and Pandis, 2009; 2010) and is called in the rest of the paper no-bSOA aging even if the O:C of bSOA does change.

In the second scheme, bSOA components are assumed to age similarly to aSOA, with their processing leading not only to changes in O:C, but also to a net reduction of their volatility. We explore all three functionalization schemes, the simple scheme (1-bin), the faster functionalization

(2-bin) and the detailed functionalization scheme (DET) together with the two bSOA aging parameterizations.

2.2.3 Fragmentation parameterizations

Fragmentation parameterizations will be examined that lead to products with lower carbon numbers than the precursor. As in Murphy et al. (2012) the bond cleavage is assumed to happen randomly and to be uniformly distributed throughout the carbon backbone. For these fragmented compounds, the functionalization kernel is applied and this will lead to increases in volatility. The fragmentation probability in our simulations is allowed to range from zero (for no fragmentation) to unity.

2.3 Combination of parameterizations

In our simulations, we used all combinations of the three functionalization schemes (1-bin, 2-bin or DET), the two bSOA aging schemes and simulated fragmentation assuming fragmentation probability *b* ranging from zero to 1. In Table 1, we summarize the parameterizations that were finally chosen for the simulations. For each of the six combinations of functionalization and bSOA aging, we assumed zero fragmentation probability (6 cases) plus we determined the fragmentation probability *b* that resulted in the minimum error for the average OA concentration. The determination of the "optimum" fragmentation probability for each case is shown in Figure C.4. For the 1-bin functionalization scheme and considering no bSOA production during aging, the OA was underpredicted for fragmentation probabilities even low as 5% so in this case the optimum *b* was equal to zero and this became the same as the 1-bin simple scheme of Murphy et al. (2012).

2.4 Evaluation of parameterizations

The prediction skill of our simulations is quantified in terms of the fractional error, the fractional bias, the absolute error, the absolute bias and the root mean square error. These are calculated using:

$$Fractional\ Error = \frac{2}{n}\sum_{i=1}^{n}\frac{|P_i - M_i|}{(P_i + M_i)}$$

$$Fractional\ Bias = \frac{2}{n}\sum_{i=1}^{n}\frac{(P_i - M_i)}{(P_i + M_i)}$$

$$Absolute\ Error = \frac{1}{n}\sum_{i=1}^{n}\left|P_i - M_i\right|$$

$$Absolute\ Bias = \frac{1}{n}\sum_{i=1}^{n}\left(P_i - M_i\right)$$

$$Root\ Mean\ Square\ Error = \sqrt{\frac{1}{n}\sum_{i=1}^{n}\left(P_i - M_i\right)^2}$$

where P_i represents the model prediction value, M_i is the corresponding measured value from the ground or above the site with the Zeppelin measurements and n is the total number of data points.

3. Results

3.1 Simple functionalization (1-bin case)

The first set of simulations used the simple functionalization scheme (1-bin), assuming negligible addition/production of bSOA during aging (no bSOA aging) and neglected fragmentation assuming that the employed functionalization scheme represents the net effect of these pathways. This case is the same as the base case of Murphy et al. (2012). In this scheme, there is a modest volatility reduction as the organic vapors react with OH. The prediction skill metrics of the model 4-hour average O:C and OA concentration against the averaged ground measurements for the seven selected days during PEGASOS 2012 campaign are summarized in Tables 2 and 3 respectively.

The average predicted diurnal variation of O:C at the ground level, is presented in Figure 2. Given the uncertainty introduced by the use of a trajectory model (e.g. a small error in the path of the air parcels can introduce significant error in the predictions), we rely on the average concentrations instead of the predictions of individual hours. Predicted O:C increased during the afternoon due to the production of secondary OA and photochemical processing (evaporation, oxidation in the gas phase and re-condensation) of the primary OA. The model predictions, agree within experimental error with the measurements, with some discrepancies in the afternoon where the model tends to overpredict O:C. They both suggest relatively oxidized OA with modest average

diurnal O:C variation. The average predicted O:C is 0.64 and the average measured is 0.58 (Table 2). The fractional error and bias for the 4-hour average O:C were less than 10%.

The predicted average O:C vertical model profile is compared to the airborne measurements, in Figure 3a. Model predictions, agree with the measurements within experimental error and both suggest an oxidized aerosol. The average predicted O:C was equal to 0.59, while the average measured O:C was 0.58. The vertical profile for both the predictions and Zeppelin measurements was relatively flat inside the lowest 1 km.

The predicted average diurnal profile of the OA particle mass concentration for the 1-bin case is shown in Figure 4. The average predicted OA is equal to 2.6 μg m^{-3} and is predicted to be higher during the night time for this specific period. The measurements suggest a relatively flat profile; however, the model predicts higher particle mass concentrations during night time due to increased levels of SOA. The average measured particle mass concentration during the same period was 2.8 μg m^{-3}. The absolute error was equal to 0.78 μg m^{-3} and the fractional bias was 12%. The anthropogenic SOA and SOA from IVOC oxidation dominate the predicted OA composition, with biogenic SOA increasing during night time. SOA-iv is predicted to contribute 36% to the total OA. Anthropogenic and biogenic SOA are predicted to account for 22 and 17% respectively and SOA-sv and POA represent around 10% each (Figure S3). The predicted average diurnal profile of the POA particle mass concentration compared to the HOA concentration from the AMS-PMF results from the ground from Sullivan et al. (2016) are also shown in Figure S4. The particle mass concentrations are always less than 0.25 μg m^{-3} and the diurnal profiles seem to agree satisfactorily. The biomass burning contribution is not present during these summer months.

The average vertical predicted profile for all Zeppelin flights is compared with the corresponding measurements in Figure 3b. The average measured OA for these periods was equal to 4.7 μg m^{-3} while the average predicted 4.2 μg m^{-3}. Model predictions are within experimental error, for altitudes lower than 700 m. The three data points at higher altitudes are all from a single flight on June 20, 2012 during which the model underpredicted the OA aloft.

3.2 Effect of functionalization scheme

Using the 2-bin simple functionalization scheme the fractional error and bias for O:C are around 10%, similar to the 1-bin parameterization. The average predicted OA is equal to 3.4 μg m^{-3} (Table 3) with similar fractional error and bias with the 1-bin case. The average volatility

distribution and O:C of OA at the ground level is shown in Figure S2. The OA mass, using this functionalization scheme is distributed towards smaller volatilities, compared to the 1-bin case, almost one bin to the left (Figure S2b), while the OA mass is distributed around similar values for the O:C with a diurnal ground average equal to 0.63 (Table 2), where 0.58 is the average for the measurements.

The detailed functionalization scheme, underpredicted the O:C, with fractional bias equal to 34% and an average O:C equal to 0.41 (Table 2), when the average measured was 0.58. This is consistent with the conclusions of Murphy et al. (2011; 2012), about the tendency of this aggressive functionalization scheme to seriously underpredict O:C. The performance of this scheme, was better for the OA mass concentration with an average predicted value equal to 3.2 μg m^{-3} (Table 3) close to the average measured value (2.8 μg m^{-3}). The OA particle mass concentration fractional bias was equal to 11% while the fractional error was 21%. In this functionalization scheme, the predicted OA has a wider distribution in the 2D space than the 2 previous schemes and lower O:C and volatilities. (Figure S2c).

3.3 Effect of bSOA production during aging

The average predicted O:C for the ground level using the 1-bin/bSOA parameterization is 0.55, which is consistent with the measured 0.58 (Table 2). The fractional error and bias of O:C are less than 10%. However, the OA concentration is overpredicted with an average value of 3.8 μg m^{-3}, compared to the measured 2.8 μg m^{-3} (Table 2). The OA particle mass concentration fractional bias and error were 26% and 30% respectively. This is consistent with the conclusions of Hermansson et al. (2014), Lane et al. (2008) and Murphy and Pandis (2009) that treating only the functionalization of bSOA while neglecting fragmentation leads to overpredictions of OA concentrations.

The same behavior was observed in the 2-bin/bSOA simulation in which PMCAMx-Trj predicted an average ground O:C equal to 0.53 with fractional bias less than 10% but overpredicted OA with an average equal to 5 μg m^{-3} and a high fractional bias of 54%. Finally, in the DET/bSOA case, the model seriously underpredicted O:C with an average value equal to 0.35 and fractional bias equal to 50% and overpredicted OA concentration with an average equal to 5.4 μg m^{-3} and a high fractional bias of 60%. In all of these cases, addition of significant later generation bSOA production leads to significant errors in the model predictions.

3.4 The role of fragmentation

To explore the role of fragmentation the 1-bin simple functionalization scheme was first used, assuming additional production of bSOA during aging combined with the fragmentation parameterization varying the fragmentation probability from zero to one. An optimum fragmentation probability equal to 0.15 was estimated (Figure S5b). The average predicted O:C for this model configuration (1-bin/bSOA/b=0.15) was equal to 0.56 in good agreement with the measurements and a fractional bias of 4% (Table 2). The average predicted OA was equal to 2.9 μg m^{-3} with a fractional bias of just 2%.

The second functionalization scheme (2-bin case) was also tested without and with bSOA aging, (2-bin and 2-bin/bSOA cases respectively). In the first case, the optimum *b* was estimated to be equal to 0.1 and in the second case, assuming bSOA aging, it was equal to 0.4 (Figures S5c and S5d) For both model configurations, the performance was satisfactory (fractional biases less than 10% and fractional errors less than 25%) for both O:C and OA mass (Table 2 and 3).

In the last test, the detailed functionalization scheme (DET case) was used. In the previous simulations, the DET and DET/bSOA parameterizations resulted in high underpredictions of the O:C and overprediction of the OA concentration for DET/bSOA case. In the DET parameterization, the optimum *b* was estimated to be equal to 0.3 and in the second case, assuming bSOA aging, it was equal to 0.7 (Figures S5e and S5f). These schemes performed well with fractional biases less than 10% and fractional errors less than 25% for OA and less than 10% for O:C.

For all three aging schemes, including suitable fragmentation schemes, resulted in satisfactory results compared to the measurements at the ground level. In Figure S4 all the parameterizations had similar POA concentrations compared to the HOA concentrations from the ground PMF-AMS measurements. The situation was similar for the Zeppelin measurements as shown in Figure S6 in the Supplementary Information. All these parameterizations resulted in similar vertical profiles of O:C and OA with similar agreement with the measurements.

3.5 Synthesis of results

The previous results suggest that there are seven aging parameterizations from those examined that reproduce well both the ground and Zeppelin measurements. These are:

- the simple functionalization scheme and assuming negligible bSOA aging (1-bin case) corresponding to the base case in Murphy et al. (2011),
- the 1-bin shift with bSOA aging and a fragmentation probability equal to 15% (1-bin/bSOA/b=0.15),
- the 2-bin shift without bSOA aging (2-bin),
- the 2-bin shift without bSOA aging and a fragmentation probability equal to 10% (2-bin/b=0.1),
- the 2-bin shift with bSOA aging and a fragmentation probability equal to 40% (2-bin/bSOA/b=0.4),
- the detailed functionalization scheme, without bSOA aging and a fragmentation probability equal to 30% (DET/b=0.3),
- the detailed functionalization scheme with bSOA aging and fragmentation probability equal to 70% (DET/bSOA/b=0.7).

Parameterizations that appear to be inconsistent with the measurements are the ones that use the detailed functionalization scheme, without any fragmentation schemes, leading to underprediction of the O:C. Parameterizations including net bSOA production during the chemical aging reactions and neglecting fragmentation were also inconsistent with the measurements resulting in overprediction of the OA levels.

These seven aging schemes predict different OA composition (Figure 5), while all perform well enough compared to the measurements. Considering the modeling uncertainty introduced by the use of a 1-D trajectory model and the corresponding measurement uncertainties, all models perform satisfactorily. While statistically, the performance of the 2-bin/bSOA/b=0.4 scheme is a little better than the others, this difference is clearly within experimental/modeling error. Anthropogenic SOA from VOCs is predicted to contribute between 14 and 27% of the total OA (Figure S3a). It is a high contributor for the simulations assuming negligible additional production of bSOA during chemical aging. The parameterization using the faster functionalization scheme (2-bin) predicts the highest percentage of 27% while the scheme with the detailed functionalization, additional bSOA production and rapid fragmentation (DET/ bSOA/b=0.7) predicts the lowest (14%).

The predicted contribution of biogenic SOA was the most variable ranging from 16 to 45% of the total OA depending on the scheme (Figure S3b). The highest contribution, as expected, was

predicted by the schemes assuming production of bSOA during aging. The highest fraction (45%) was predicted using the 2-bin shift functionalization parameterization and fragmentation by 40% (2-bin/bSOA/b=0.4. The lower bSOA mass concentrations were predicted by the four schemes assuming negligible net bSOA production during aging.

SOA from the oxidation of intermediate volatility compounds varied between 19 and 36% depending on the model (Figure S3c). The lowest contributions were predicted by the simulations in which the bSOA mass concentration was high. The primary OA varied from 5 to 6%, the OA from long range transport from 6 to 8%, and the SOA from evaporation of the primary and subsequent oxidation from 7 to 11%.

These results are encouraging because the various parameterizations even if they are quite different they give a rather consistent picture (with exception of the picture of the bSOA maybe) about the various pathways contributing to the OA levels in this area. Additional constraining of these schemes will require applications of the corresponding models in other areas, additional measurements, and probably additional laboratory studies.

3.6 The role of vaporization enthalpy

The vaporization enthalpy is a physical property that has always been assumed in chemical transport models with values ranging from very low as 20 to even 200 kJ mol^{-1} that have been suggested after constraining these values with experimental data (Stanier et al., 2007; Offenberg et al., 2017). In our model, three different effective vaporization enthalpies equal to 30, 75 and 150 kJ mol^{-1} were assumed and used together with the simple functionalization scheme (1-bin case). All three simulations, predicted the same flat diurnal profile for both the O:C and OA concentration, with differences less than 20%, mostly in the first hours of the day (Figure 6a and b). The predictions of the scheme with the higher vaporization enthalpy tend to be a little closer to the ground measurements of O:C. As vaporization enthalpy increased, the predicted O:C decreased and OA concentration increased (Table S1) However, the differences were small with the average O:C ranging from 0.59 for the 150 kJ mol^{-1} case to 0.64 for the 30 kJ mol^{-1} case, while the measured average value was 0.58. The fractional biases for O:C were similar ranging from 2% for a vaporization enthalpy equal to 150 kJ mol^{-1} to 10% for 30 kJ mol^{-1}. The results for the OA concentration were similar.

The comparison of the model predictions with the vertical profiles from the Zeppelin measurements showed similar results (Figure 6c and d). The predicted vertical profiles of O:C and OA particle mass concentration were once more not that sensitive to the assumed effective vaporization enthalpy. This lack of sensitivity can be explained by the intricate interplay between the changes in partitioning of the semi-volatile compounds and their gas-phase chemical aging reactions. The sensitivity of the vaporization enthalpy was examined with all aging mechanisms and the conclusions were the same.

For values of ΔH_{vap} that favor the partitioning of the OA components to the gas phase the resulting decrease in OA concentrations is partially offset by an acceleration of the gas-phase chemical aging reactions and the additional SOA production. Vice-versa for ΔH_{vap} values that favor the partitioning to the particulate phase the resulting OA increase is balanced by a reduction in the aging rate.

4. Conclusions

The effects of the parameterization of the chemical aging processes of atmospheric organic compounds on organic aerosol (OA) particle mass concentration and chemical composition were investigated by using different formulations of the two-dimensional Volatility Basis Set (2D-VBS) together with ground and airborne measurements in the Po Valley in Italy.

We applied firstly the simple aging mechanism of the base case (Murphy et al., 2012), presented here as the 1-bin case. The predictions of the model were satisfactory, both at the ground and aloft, within experimental variability and with fractional biases for the 4-hour average O:C and OA concentration around 10%. The average diurnal POA concentration was similar to the HOA concentration from the PMF-AMS ground measurements with concentrations less than 0.25 $\mu g\ m^{-3}$. The vertical profile for both predictions of the 1-bin case and Zeppelin measurements was relatively flat inside the lowest 1 km and the diurnal variation in O:C ratio was modest. They both suggested a relatively oxidized OA for the Po Valley, Italy, with an average O:C around 0.6. Anthropogenic SOA and SOA from intermediate volatility compounds oxidation dominated the predicted OA composition based on this parameterization.

Seven aging schemes (out of more than a hundred tested), with different assumed functionalization algorithms, bSOA aging and fragmentation were found to reproduce well the ground and Zeppelin O:C and OA measurements. Anthropogenic SOA from VOCs was predicted

to contribute between 15 and 25% of the total OA and SOA from the oxidation of intermediate volatility compounds oxidation between 20 and 35%. The contribution of biogenic SOA varied from 15 to 45%, depending on the parameterization scheme. POA was around 5%, with almost similar average diurnal profiles between the different parameterizations and similar to the HOA concentrations from the PMF-AMS ground measurements. The OA from long range transport varied from 6 to 8% and the SOA from evaporation of the primary and subsequent oxidation from 7 to 11%. These results are encouraging because despite the uncertainty introduced by the different schemes, their predictions about source contributions are relatively robust.

Addition of bSOA produced during the corresponding chemical aging reactions in the functionalization-only schemes resulted in overpredictions of the OA mass concentration. Addition of significant fragmentation (fragmentation probabilities ranging from 15 to 70%) was necessary to balance this additional source. This is clearly a topic that deserves additional research both in the laboratory and in the field.

There was also surprising low sensitivity of predicted OA particle mass concentration and O:C both at the ground and aloft to enthalpy of vaporization. Using three different vaporization enthalpies equal to 30, 75 and 150 kJ mol^{-1}, the model predictions showed a very similar flat diurnal profile for O:C and OA particle mass concentration at the ground with differences less than 20% and being within experimental variability. Similar were the conclusions for the vertical profiles of the model in comparison to the Zeppelin measurements. The interplay between the partitioning of the compounds and the chemical aging reactions as well as the small temperature sensitivity, for altitudes until 600 m might explain this small sensitivity to vaporization enthalpy. There was some weak evidence though that the higher values (like 150 kJ mol^{-1}) are in better agreement with the O:C observations at the ground and aloft. Probably this low sensitivity is also a feature of analyzing within the boundary layer during only the summer. Future work with three-dimensional models and measurements with high altitude predictions and/or annual simulations with wintertime predictions may be useful.

Acknowledgements

This research was supported by the PEGASOS project funded by the European Commission under the Framework Program 7 (FP7-ENV-2010-265148) and the grant 1455244 from the US National Science Foundation.

References

Caiazzo, F., Ashok, A., Waitz, I. A., Yim, S. H. L. and Barrett, S. R. H.: Air pollution and early deaths in the United States. Part I: Quantifying the impact of major sectors in 2005, Atmospheric Environment, 79, 198–208, 2013.

Cappa, C. D. and Wilson, K. R.: Multi-generation gas-phase oxidation, equilibrium partitioning, and the formation and evolution of secondary organic aerosol, Atmos. Chem. Phys., 12, 9505–9528, 2012.

Cappa, C. D., Zhang, X., Loza, C. L., Craven, J. S., Yee, L. D., and Seinfeld, J. H.: Application of the Statistical Oxidation Model (SOM) to secondary organic aerosol formation from photooxidation of C12 alkanes, Atmos. Chem. Phys., 13, 1591–1606, 2013.

Carter, W. P. L.: Programs and files implementing the SAPRC-99 mechanism and its associated emissions processing procedures for Models-3 and other regional models, 31 January, 2000.

Chacon-Madrid, H. J. and Donahue, N. M.: Fragmentation vs. functionalization: chemical aging and organic aerosol formation, Atmos. Chem. Phys., 11, 10553–10563, 2011.

Donahue, N. M., Robinson, A. L., Stanier, C. O., and Pandis, S. N.: Coupled partitioning, dilution, and chemical aging of semivolatile organics, Environ. Sci. Technol., 40, 2635-2643, 2006.

Donahue, N. M., Kroll, J. H., Pandis, S. N., and Robinson, A. L.: A two-dimensional volatility basis set: 1. organic-aerosol mixing thermodynamics, Atmos. Chem. Phys., 11, 3303–3318, 10.5194/acp-11-3303-2011, 2011.

Donahue, N. M., Epstein, S. A., Pandis, S. N., and Robinson, A. L.: A two-dimensional volatility basis set – Part 2: Diagnostics of organic-aerosol evolution, Atmos. Chem. Phys., 12, 615–634, 10.5194/acp-12-615-2012, 2012a.

Donahue, N. M., Henry, K. M., Mentel, T. F., Kiendler-Scharr, A., Spindler, C., Bohn, B., Brauers, T., Dorn, H. P., Fuchs, H., Tillmann, R., Wahner, A., Saathoff, H., Naumann, K. H., Möhler, O., Leisner, T., Müller, L., Reinnig, M. C., Hoffmann, T., Salo, K., Hallquist, M., Frosch, M., Bilde, M., Tritscher, T., Barmet, P., Baltensperger, U.: Aging of biogenic secondary organic aerosol via gas-phase OH radical reactions, Proc. Natl. Acad. Sci., 109, 13503–13508, 2012b.

Draxler, R., Stunder, B., Rolph, G., Stein, A., and Taylor, A.: HYSPLIT4 User's Guide, NOAA Silver Spring, MD, 231, 2009.

Fountoukis C., Racherla P. N., Denier van der Gon H. A. C., Polymeneas P., Charalampidis P. E., Pilinis C., Wiedensohler A., Dall'Osto M., O'Dowd C., and S. N. Pandis: Evaluation of a three-dimensional chemical transport model (PMCAMx) in the European domain during the EUCAARI May 2008 campaign, Atmos. Chem. Phys., 11, 10331-10347, 10.5194/acp-11-10331-2011, 2011.

Gilardoni, S., Vignati, E., Cavalli, F., Putaud, J. P., Larsen, B. R., Karl, M., Stenstrom, K., Genberg, J., Henne, S., and Dentener, F.: Better constraints on sources of carbonaceous aerosols using a combined ^{14}C - macro tracer analysis in a European rural background site, Atmos. Chem. Phys., 11, 5685–5700, 2011.

Guenther, A., Karl, T., Harley, P., Wiedinmyer, C., Palmer, P. I., and Geron, C.: Estimates of global terrestrial isoprene emissions using MEGAN (Model of Emissions of Gases and Aerosols from Nature), Atmos. Chem. Phys., 6, 3181–3210, 10.5194/acp-6-3181-2006, 2006.

Hermansson, E., Roldin, P., Rusanen, A., Mogensen, D., Kivekäs, N., Väänänen, R., Boy, M., and Swietlicki, E.: Biogenic SOA formation through gas-phase oxidation and gas-to-particle partitioning – a comparison between process models of varying complexity, Atmos. Chem. Phys., 14, 11853–11869, 2014.

IPCC (Intergovernmental Panel on Climate Change): Climate Change 2014: Mitigation of Climate Change. Contribution of Working Group III to the Fifth Assessment Report of the Intergovernmental Panel on Climate Change, Cambridge University Press, Cambridge, UK and New York, 2014.

Jathar, S. H., Cappa, C. D., Wexler, A. S., Seinfeld, J. H. and Kleeman, M. J.: Multi-generational oxidation model to simulate secondary organic aerosol in a 3-D air quality model, Geosci. Model Dev., 8, 2553-2567, 2015.

Jimenez, J. L., Canagaratna, M. R., Donahue, N. M., Prévôt, A. S. H., Zhang, Q., Kroll, J. H., DeCarlo, P. F., Allan, J. D., Coe, H., Ng, N. L., Aiken, A. C., Docherty, K., Ulbrich, I., Grieshop, A.P., Robinson, A. L., Duplissy, J., Smith, J. D., Wilson, K. R., Lanz, V. A., Hueglin, C., Sun, Y. L., Tian, J., Laaksonen, A., Raatikainen, T., Rautiainen, J., Vaattovaara, P., Ehn, M., Kulmala, M., Tomlinson, J. M., Collins, D. R., Cubison, M. J., Dunlea, E., Huffman, J. A., Onasch, T. B., Alfarra, M. R., Williams, P., Bower, K., Kondo, Y., Schneider, J., Drewnick, F., Borrmann, S., Weimer, S., Demerjian, K., Salcedo, D., Cottrell, L., Griffin, R. J., Takami, A., Miyoshi, T., Hatakeyama, S., Shimono, A., Sun, J. Y., Zhang,

Y. M., Dzepina, K., Kimmel, J. R., Sueper, D., Jayne, J. T., Herndon, S. C., Trimborn, A., Williams, L. R., Wood, E. C., Middlebrook, A. M., Kolb, C. E., Baltensperger, U., and Worsnop, D. R.: Evolution of organic aerosols in the atmosphere, Science, 326, 1525–1529, 2009.

Kulmala, M., Asmil, A., Lappalainen, H. K., Carslaw, K. S., Poschl, U., Baltensperger, U., Hoy, O., Brenquier, J.-L., Pandis, S. N., Facchini, M. C., Hansson, H. C., Wiedensohler, A., and O'Dowd, C. D.: Introduction: European Integrated Project on Aerosol Cloud Climate and Air Quality interactions (EUCAARI) – integrating aerosol research from nano to global scales, Atmos. Chem. Phys., 9, 2825–2841, 10.5194/acp-9-2825-2009, 2009.

Lane, T. E., Donahue, N. M., and Pandis, S. N.: Simulating secondary organic aerosol formation using the volatility basis-set approach in a chemical transport model, Atmos. Environ., 42, 7439–7451, 2008.

Murphy, B. N. and Pandis, S. N.: Simulating the formation of semivolatile primary and secondary organic aerosol in a regional chemical transport model, Environ. Sci. Technol., 43, 4722–4728, 2009.

Murphy, B. N. and Pandis, S. N.: Exploring summertime organic aerosol formation in the eastern United States using a regional-scale budget approach and ambient measurements, J. Geophys. Res., 115, D24216, 10.1029/2010jd014418, 2010.

Murphy, B. N., Donahue, N. M., Fountoukis, C., and Pandis, S. N.: Simulating the oxygen content of ambient organic aerosol with the 2D volatility basis set, Atmos. Chem. Phys., 11, 7859-7873, 10.5194/ acp-11-7859-7873-2011, 2011.

Murphy, B. N., Donahue, N. M., Fountoukis, C., Dall'Osto, M., Dowd, C. O., Kiendler-Scharr, A., and Pandis, S. N.: Functionalization and fragmentation during ambient organic aerosol aging: application of the 2-D volatility basis set to field studies, Atmos. Chem. Phys., 12, 10797-10816, 10.5194/ acp-12-10797-10816-2012, 2012.

Murphy, B. N., Donahue, N. M., Robinson, A. L., and Pandis, S. N.: A naming convention for atmospheric organic aerosol, Atmos. Chem. Phys., 14, 5825–5839, doi:10.5194/acp-14-5825-2014, 2014.

Ng, N. L., Kroll, J. H., Keywood, M. D., Bahreini, R., Varutbangkul, V., Flagan, R. C., and Seinfeld, J. H.: Contribution of first- versus second-generation products to secondary

organic aerosols formed in the oxidation of biogenic hydrocarbons, Environ. Sci. Technol., 40, 2283–2297, 2006.

O'Dowd, C. D., Langmann, B., Varghese, S., Scannell, C., Ceburnis, D., and Facchini, M. C.: A combined organic-inorganic sea spray source function, Geophys. Res. Lett., 35, L01801, 10.1029/2007GL030331, 2008.

Offenberg, J. H., Lewandowski, M., Kleindienst, T. E., Docherty, K. S., Jaoui, M., Krug, J., Riedel, T. P., and Olson D. A.: Predicting Thermal Behavior of Secondary Organic Aerosols, Environ. Sci. Technol., 51, 9911-9919, 2017.

Pandis S. N., Harley R. A., Cass G. R. and Seinfeld J. H.: Secondary Organic Aerosol Formation and Transport, Atmos. Environ., 26, 2266-2282, 1992.

Pathak, R. K., Presto, A. A., Lane, T. E., Stanier, C. O., Donahue, N. M., and Pandis, S. N.: Ozonolysis of α-pinene: parameterization of secondary organic aerosol mass fraction, Atmos. Chem. Phys., 7, 3811–3821, 10.5194/acp-7-3811-2007, 2007.

Pope, C. A., III, Ezzati, M. and Dockery, D. W.: Fine-particulate air pollution and life expectancy in the United States, New England Journal of Medicine, 360, 376–386, 2009.

Sheehan, P. E. and Bowman, F. M.: Estimated effects of temperature on secondary organic aerosol concentrations, Environ. Sci. Technol., 35, 2129–2135, 2001.

Shrivastava, M., Fast, J., Easter, R., Gustafson Jr., W. I., Zaveri, R. A., Jimenez, J. L., Saide, P., and Hodzic, A.: Modeling organic aerosols in a megacity: comparison of simple and complex representations of the volatility basis set approach, Atmos. Chem. Phys., 11, 6639–6662, 2011.

Sofiev, M., Lanne, M., Vankevich, R., Prank, M., Karppinen, A., and Kukkonen, J.: Impact of wild-land fires on European air quality in 2006–2008, Modeling, Monitoring and Management of Forest Fires, WIT Trans. Ecol. Envir., 119, 353–361, 2008a.

Sofiev, M., Vankevich, R., Lanne, M., Koskinen, J., and Kukkonen, J.: On integration of a Fire Assimilation System and a chemical transport model for near-real-time monitoring of the impact of wild-land fires on atmospheric composition and air quality, Modeling, Monitoring and Management of Forest Fires, WIT Trans. Ecol. Envir., 119, 343–351, 2008b.

Stanier, C. O., Pathak, R. K., and Pandis, S. N.: Measurements of the volatility of aerosols from α-pinene ozonolysis, Environ. Sci.Technol., 41, 2756–2763, 2007.

Stanier, C. O., Donahue, N., Pandis, S. N.: Parameterization of secondary organic aerosol mass fractions from smog chamber data, Atmos. Environ., 42, 2276–2299, 2008.

Sullivan, A. P., Hodas, N., Turpin, B. J., Skog, K., Keutsch, F. N., Gilardoni, S., Paglione, M., Rinaldi, M., Decesari, S., Facchini, M. C., Poulain, L., Herrmann, H., Wiedensohler, A., Nemitz, E., Twigg, M. M., and Collett Jr., J. L.: Evidence for ambient dark aqueous SOA formation in the Po Valley, Italy, Atmos. Chem. Phys., 16, 8095-8108, 2016.

Szidat, S., Jenk, T. M., Synal, H.-A., Kalberer, M., Wacker, L., Hajdas, I., Kasper-Giebl, A., and Baltensperger, U.: Contributions of fossil fuel, biomass-burning, and biogenic emissions to carbonaceous aerosols in Zurich as traced by 14C, J. Geophys. Res., 111, D07206, 10.1029/2005JD006590, 2006.

Tritscher, T., Dommen, J., DeCarlo, P. F., Barmet, P. B., Pra-plan, A. P., Weingartner, E., Gysel, M., Prévôt, A. S. H., Riipinen, I., Donahue, N. M., and Baltensperger, U.: Volatility and hygroscopicity of aging secondary organic aerosol in a smog chamber, Atmos. Chem. Phys., 11, 11477-11496, 2011.

Visschedijk, A. J., Zandveld, P., and Denier van der Gon, H. A. C.: TNO Report 2007 A-R0233/B: A high resolution gridded European emission database for the EU integrated project GEMS, Organization for Applied Scientific Research, The Netherlands, 2007.

Yttri, K. E., Simpson, D., Nøjgaard, J. K., Kristensen, K., Genberg, J., Stenström, K., Swietlicki, E., Hillamo, R., Aurela, M., Bauer, H., Offenberg, J. H., Jaoui, M., Dye, C., Eckhardt, S., Burkhart, J. F., Stohl, A., and Glasius, M.: Source apportionment of the summer time carbonaceous aerosol at Nordic rural background sites, Atmos. Chem. Phys., 11, 13339-13357, 2011.

Zhang, Q., Jimenez, J. L., Canagaratna, M. R., Allan, J. D., Coe, H., Ulbrich, I., Alfarra, M. R., Takami, A., Middlebrook, A. M., Sun, Y. L., Dzepina, K., Dunlea, E., Docherty, K., De-Carlo, P. F., Salcedo, D., Onasch, T., Jayne, J. T., Miyoshi, T., Shimono, A., Hatakeyama, S., Takegawa, N., Kondo, Y., Schneider, J., Drewnick, F., Borrmann, S., Weimer, S., Demerjian, K., Williams, P., Bower, K., Bahreini, R., Cottrell, L., Griffin, R. J., Rautiainen, J., Sun, J. Y., Zhang, Y. M., and Worsnop, D. R.: Ubiquity and dominance of oxygenated species in organic aerosols in anthropogenically-influenced Northern Hemisphere midlatitudes, Geophys. Res. Lett., 34, L13801, 10.1029/2007GL029979, 2007.

Zhang, Q. J., Beekmann, M., Drewnick, F., Freutel, F., Schneider, J., Crippa, M., Prévôt, A. S. H., Baltensperger, U., Poulain, L., Wiedensohler, A., Sciare, J., Gros, V., Borbon, A., Colomb, A., Michoud, V., Doussin, J. F., Denier van der Gon, H. A. C., Haeffelin, M., Dupont, J. C., Siour, G., Petetin, H., Bessagnet, B., Pandis, S. N., Hodzic, A., Sanchez, O., Honoré, C., and Perrussel, O.: Formation of organic aerosol in the Paris region during the MEGAPOLI summer campaign: evaluation of the volatility-basis-set approach within the CHIMERE model, Atmos. Chem.Phys., 13, 5767–5790, 2013.

Zhao, B., Wang, S., Donahue, N. M., Chuang, W., Hildebrandt-Ruiz, L., Ng, N. L., Wang, Y., and Hao, J.: Evaluation of one-dimensional and two-dimensional volatility basis sets in simulating the aging of secondary organic aerosol with smog-chamber experiments, Environ. Sci. Technol., 49, 2245–2254, 2015.

Atmos. Chem. Phys. Discuss., https://doi.org/10.5194/acp-2018-22
Manuscript under review for journal Atmos. Chem. Phys.
Discussion started: 22 January 2018

Table 1. Characteristics of the different parameterizations used in our simulations.

Parameterization Name	Functionalization scheme	bSOA increase during aging	Fragmentation probability	Comments
1-bin	1-bin	No	b=0	
1-bin/bSOA	1-bin	Yes	b=0	
1-bin	1-bin	No	b=0-1	Optimum for b=0, same as 1-bin case
1-bin/bSOA/b=0.15	1-bin	Yes	b=0-1	Optimum for b=0.15
2-bin	2-bin	No	b=0	
2-bin/bSOA	2-bin	Yes	b=0	
2-bin/b=0.1	2-bin	No	b=0-1	Optimum for b=0.1
2-bin/bSOA/b=0.4	2-bin	Yes	b=0-1	Optimum for b=0.4
DET	DET	No	b=0	
DET/bSOA	DET	Yes	b=0	
DET/b=0.3	DET	No	b=0-1	Optimum for b=0.3
DET/bSOA/b=0.7	DET	Yes	b=0-1	Optimum for b=0.7

Atmos. Chem. Phys. Discuss., https://doi.org/10.5194/acp-2018-22
Manuscript under review for journal Atmos. Chem. Phys.
Discussion started: 22 January 2018

Table 2. Performance metrics of different parameterizations during the PEGASOS campaign for ground O:C measurements. The measured average O:C was 0.58.

2D-VBS Parameterization	Predicted Average	Fractional Error	Fractional Bias	Absolute Error	Absolute Bias	Root Mean Square Error
1-bin	0.64	0.1	0.09	0.06	0.06	0.08
1-bin/bSOA	0.55	0.07	-0.06	0.04	-0.03	0.05
1-bin/bSOA/b=0.15	0.56	0.07	-0.04	0.04	-0.02	0.05
2-bin	0.63	0.09	0.08	0.05	0.05	0.06
2-bin/bSOA	0.53	0.10	-0.10	0.05	-0.05	0.06
2-bin/b=0.1	0.65	0.12	0.11	0.07	0.07	0.08
2-bin/bSOA/b=0.4	0.58	0.05	0.0	0.03	0.00	0.04
DET	0.41	0.34	-0.34	0.17	-0.17	0.17
DET/bSOA	0.35	0.49	-0.49	0.23	-0.23	0.23
DET/b=0.3	0.57	0.05	-0.03	0.03	-0.01	0.04
DET/bSOA/b=0.7	0.62	0.08	0.06	0.05	0.04	0.05

Atmos. Chem. Phys. Discuss., https://doi.org/10.5194/acp-2018-22
Manuscript under review for journal Atmos. Chem. Phys.
Discussion started: 22 January 2018

Table 3. Performance metrics of different parameterizations during the PEGASOS campaign for ground OA mass measurements. The measured average organic aerosol concentration was 2.8 μg m^{-3}.

2D-VBS Parameterization	Predicted Average (μg m^{-3})	Fractional Error	Fractional Bias	Absolute Error (μg m^{-3})	Absolute Bias (μg m^{-3})	Root Mean Square Error (μg m^{-3})
1-bin	2.6	0.29	-0.12	0.78	-0.25	0.89
1-bin/bSOA	3.8	0.3	0.26	1.09	0.97	1.50
1-bin/bSOA/b=0.15	2.9	0.27	-0.02	0.79	0.05	0.96
2-bin	3.4	0.23	0.16	0.76	0.56	1.06
2-bin/bSOA	5	0.54	0.54	2.21	2.21	2.53
2-bin/b=0.1	2.9	0.22	0.02	0.67	0.11	0.85
2-bin/bSOA/b=0.4	3.1	0.22	0.07	0.71	0.3	0.96
DET	3.2	0.21	0.11	0.67	0.4	0.93
DET/bSOA	5.4	0.6	0.6	2.53	2.53	2.80
DET/b=0.3	2.9	0.22	0.01	0.66	0.1	0.84
DET/bSOA/b=0.7	2.9	0.24	0.02	0.71	0.12	0.87

Atmos. Chem. Phys. Discuss., https://doi.org/10.5194/acp-2018-22
Manuscript under review for journal Atmos. Chem. Phys.
Discussion started: 22 January 2018

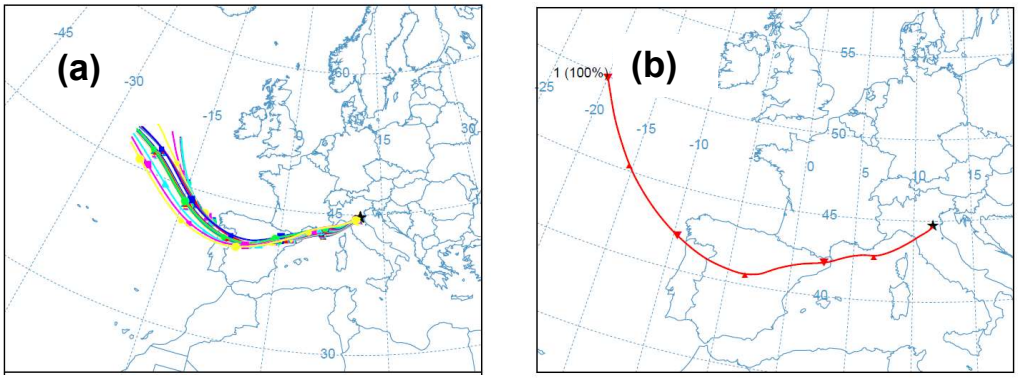

Figure 1. (a) The ensemble of 20 trajectories calculated by HYSPLIT for air parcels arriving at the San Pietro Capofiume site on 8 July 2012 at 3:00 LT and **(b)** the ensemble average trajectory calculated by the HYSPLIT clustering utility.

Atmos. Chem. Phys. Discuss., https://doi.org/10.5194/acp-2018-22
Manuscript under review for journal Atmos. Chem. Phys.
Discussion started: 22 January 2018

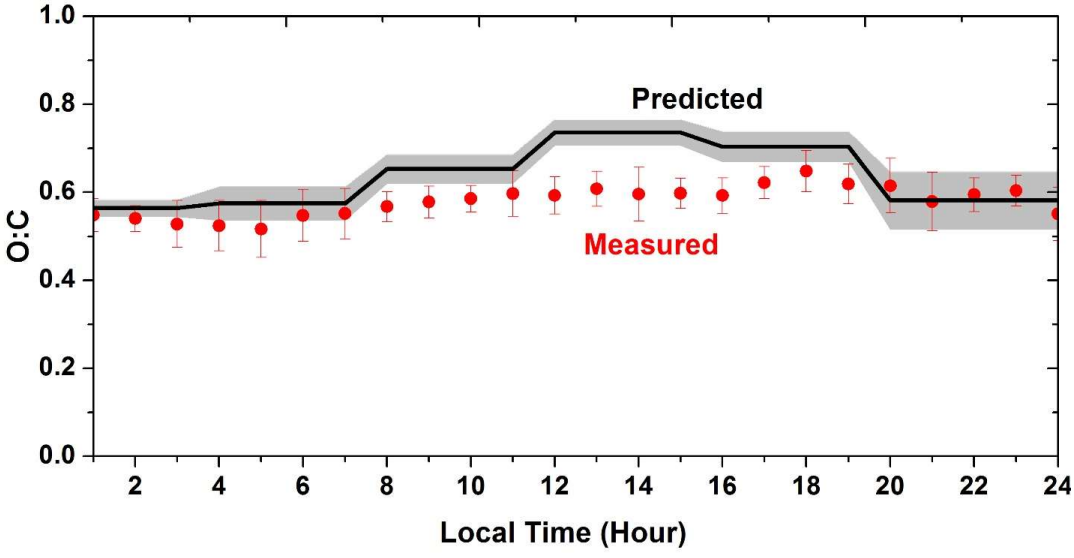

Figure 2. Average O:C diurnal evolution at the ground level in San Pietro Capofiume for the 1-bin simulation. The black line shows the 4-hour model predictions (6 plateaus from 6 hours of model predictions) and the shaded area corresponds to one standard deviation. The red symbols represent the ground AMS measurements and the error bars correspond to one standard deviation.

Atmos. Chem. Phys. Discuss., https://doi.org/10.5194/acp-2018-22
Manuscript under review for journal Atmos. Chem. Phys.
Discussion started: 22 January 2018

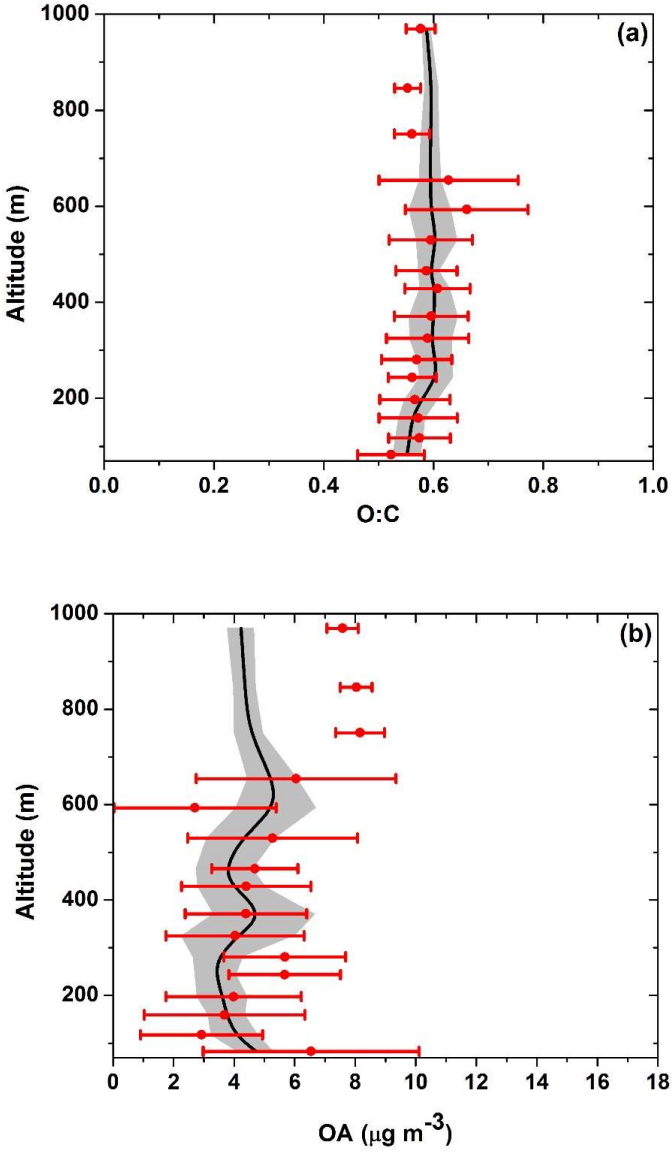

Figure 3. Average vertical predicted and measured (1-bin case) **(a)** O:C ratio and **(b)** organic aerosol mass concentration for all the Zeppelin measurements over Po Valley. The black line shows the model predictions and the shaded areas the standard deviation. The red symbols represent the AMS Zeppelin measurements and the error bars correspond to one standard deviation.

Atmos. Chem. Phys. Discuss., https://doi.org/10.5194/acp-2018-22
Manuscript under review for journal Atmos. Chem. Phys.
Discussion started: 22 January 2018

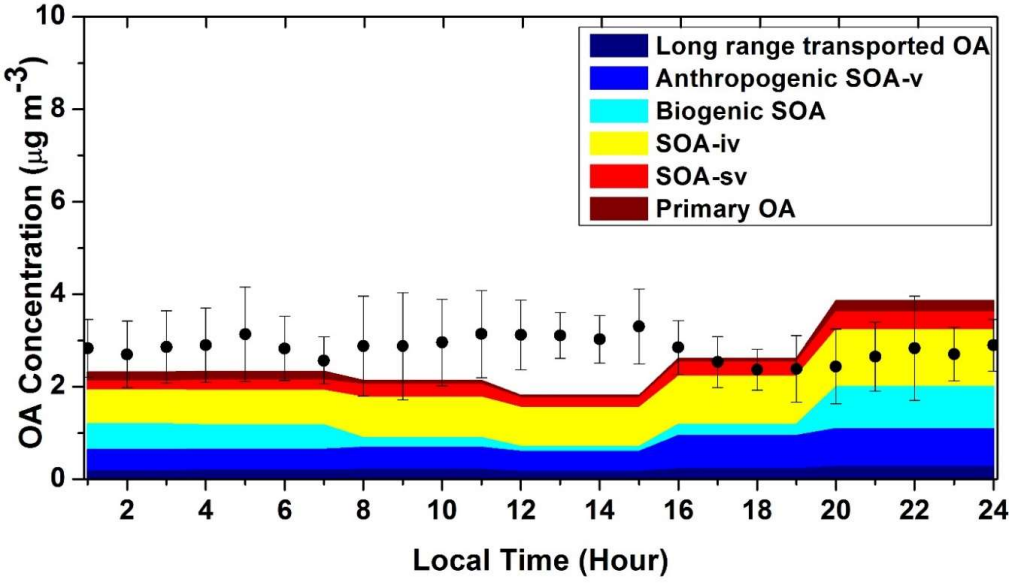

Figure 4. Average diurnal profile at the ground level OA in San Pietro Capofiume (1-bin case). With dark blue we represent the OA from long range transport, with blue the anthropogenic SOA produced during the oxidation of anthropogenic VOCs (aSOA-v), with cyan the biogenic SOA (bSOA), with yellow the SOA from oxidation of intermediate volatility compounds (SOA-iv), with red the SOA from the oxidation of semivolatile OA (SOA-sv) and finally with dark red the fresh primary organic aerosol (FPOA). The ground AMS measurements are shown with black symbols and the error bars correspond to one standard deviation.

Atmos. Chem. Phys. Discuss., https://doi.org/10.5194/acp-2018-22
Manuscript under review for journal Atmos. Chem. Phys.
Discussion started: 22 January 2018

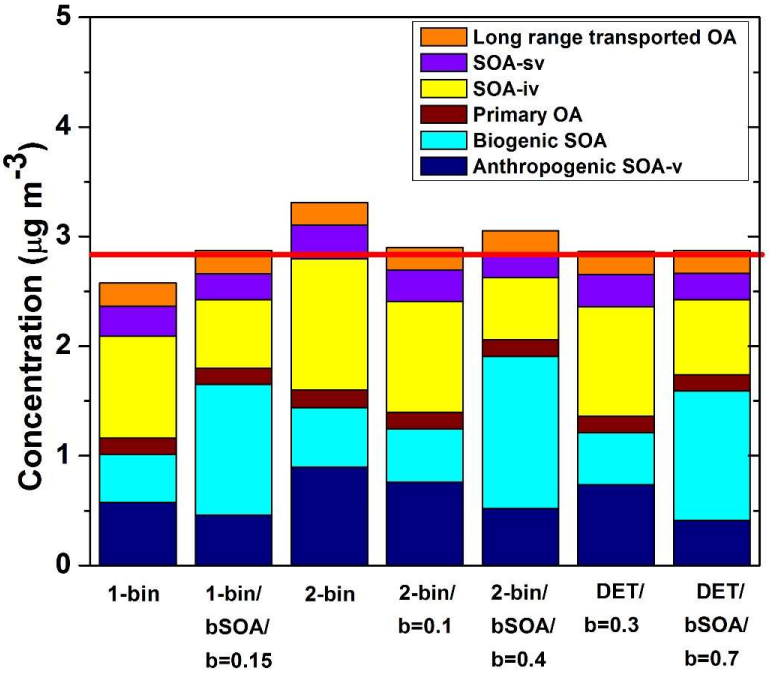

Figure 5. Predicted OA composition for the schemes with good performance for San Pietro Capofiume. The red line indicates the average measured OA equal to 2.8 μg m^{-3}.

Atmos. Chem. Phys. Discuss., https://doi.org/10.5194/acp-2018-22
Manuscript under review for journal Atmos. Chem. Phys.
Discussion started: 22 January 2018

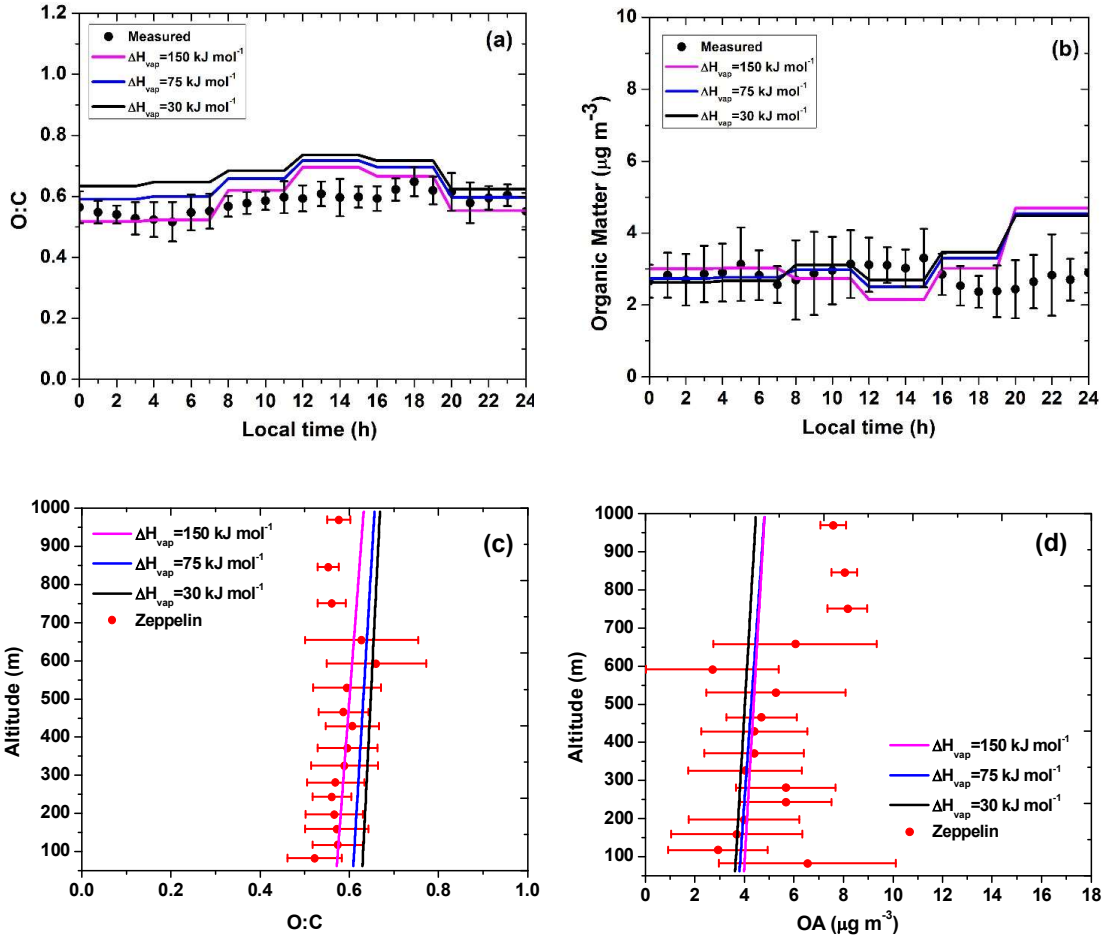

Figure 6. Diurnally average (a) O:C ratios and (b) organic aerosol mass concentrations. Average vertical organic aerosol (c) O:C and (d) organic aerosol mass concentrations assuming in the model ΔH_{vap}= 30 kJ mol^{-1} (black line), ΔH_{vap}= 75 kJ mol^{-1} (blue line), and ΔH_{vap}= 150 kJ mol^{-1} (magenta line) for the Po Valley in Italy. The black symbols show the ground AMS measurements. The red symbols show the Zeppelin measurements. The error bars represent one standard deviation.